

Tribocorrosion and Electrochemical Behavior of DIN 1.4110 Martensitic Stainless Steels After Cryogenic Heat Treatment

Leandro Brunholi Ramos^{a}, Leonardo Simoni^a, Rafael Gomes Mielczarski^a, Maria Rita Ortega Vega^a,
Roberto Moreira Schroeder^a, Célia de Fraga Malfatti^a*

*^a Corrosion Research Laboratory - LAPEC, Federal University of Rio Grande do Sul - UFRGS,
Av. Bento Gonçalves 9500, Block 4, BLDG 43 427, 2nd FL, Porto Alegre, RS, Brazil*

Received: May 02, 2016; Revised: December 15, 2016; Accepted: January 25, 2017

DIN 1.4110 martensitic stainless steel is largely used in the cutlery industry due to its high corrosion resistance associated with high mechanical resistance. However, when this material works under corrosion and wear conditions at the same time, their synergistic effect can accelerate the degradation process of the alloy. Cryogenic heat treatments have been proposed to improve the dimensional stability and mechanical properties, since they minimize the amount of retained austenite. The aim of this work is to study the effect of deep cryogenic heat treatment at $-80\text{ }^{\circ}\text{C}$ and at $-196\text{ }^{\circ}\text{C}$ on the corrosion resistance and tribocorrosion behavior of DIN 1.4110 martensitic stainless steel. The microstructure, hardness, corrosion resistance and tribocorrosion behavior were evaluated. Although the heat-treated samples presented higher hardness and lower corrosion current density (i_{corr}) compared to samples in spheroidized condition, their material removal under tribocorrosion conditions increased, which demonstrated the synergy between corrosion and wear.

Keywords: *DIN 1.4110; Cryogenic heat treatments; Corrosion; Tribocorrosion*

1. Introduction

DIN 1.4110 martensitic stainless steel is used extensively in general cutlery (i.e. food processing blades and cutting tools) due to its high corrosion and mechanical resistance, as well as high hardness and wear resistance¹. This steel has a chemical composition similar to that of AISI 420 martensitic stainless steel, although its carbon content is higher. This alloy has an arrangement in carbon and chrome content to extend the “gamma loop”; when heated to the austenitic phase field and fast cooled, it produces a martensitic microstructure - a metastable microstructure that confers high hardness and wear resistance.

As spheroidized, DIN 1.4110 stainless steel shows a microstructure consisting of dispersed spheroidized carbides in a matrix of ferrite, resulting in an average hardness of 200 HV².

Martensitic stainless steel (AISI 420, AISI 410, AISI 416 and AISI 403, for example) shows good corrosion resistance compared to low alloy steels. However, the martensitic stainless steel corrosion resistance is lower than that of austenitic and ferritic steels. In particular, super-ferritic stainless steels present an enhancement of their corrosion resistance because of the high chromium content that works as a ferrite stabilizer³. Hardness and wear resistance can be crucial for certain applications such as gas turbine blades⁴. Following this trend, some studies have proposed the plasma nitriding process and the addition of alloying elements such as nitrogen, nickel and molybdenum to increase corrosion and wear resistance^{3,5-7}.

DIN 1.4110 martensitic stainless steel is largely used in the cutlery industry as cutting blades, which has motivated studies aiming to characterize and improve the tribological properties of these materials. The combined corrosion-wear effect can result in serious problems for materials under wear and corrosion conditions. If wear (mechanical effect) and corrosion (chemical or electrochemical effect) processes act simultaneously, it can lead to an enhanced level of material loss due to their synergic effect⁸.

The studied material does not present a 100% martensitic microstructure after conventional quenching due to its high alloying elements and carbon content⁹. However, cryogenic treatments are an option to increase martensite content after conventional quenching. As a consequence of the greater content of martensite, these treatments confer to the steel an increase in dimensional stability, hardness, and wear and fatigue resistance¹⁰⁻¹³. Cryogenic treatments are usually carried out at $-80\text{ }^{\circ}\text{C}$ and $-196\text{ }^{\circ}\text{C}$, corresponding to dry ice sublimation temperature and liquid nitrogen boiling temperature, respectively¹². Such treatments can influence the amount of retained austenite inside the steel, considering that the lower temperature of the treatment, depending on the steel martensite finish (M_f) line, induces the transformation of a higher amount of austenite to martensite; consequently, a lower fraction of retained austenite will remain in the steel. This can influence the steel's properties, since it is softer than martensite, reduces the dimensional precision of the components, and also shows a different corrosion behavior compared to the martensitic matrix.

* e-mail: leandrobrunholi.lbr@gmail.com

Tempering temperature also plays an important role in retained austenite content. Besides stress relieving and hardness decrease, using an appropriate tempering temperature can lead to a decrease of its fraction, since this treatment transforms the retained austenite into ferrite and cementite¹⁴.

The main objective of this study is to interrogate the influence of cryogenic heat treatment (-80 °C and -196 °C) on the electrochemical and tribocorrosion behavior of DIN 1.4110 martensitic stainless steel.

2. Experimental

2.1. Materials

The material tested was DIN 1.4110 martensitic stainless steel, with chemical compositions shown in Table 1.

Table 1. Chemical composition in % weight of DIN 1.4110 martensitic stainless steel of work material.

C	Cr	Si	Mn	Mo	S	P	Fe
0.58	14.39	0.36	0.35	0.62	<0.001	<0.018	Balance

Samples were cut from LASER in a square section of 50 mm x 50 mm, and 3.5 mm thickness. The flat surfaces of the samples were wet-sanded using silicon carbide papers from 180 grit down to 600 grit.

All the tests were carried out in triplicate to ensure reproducibility.

2.2. Heat treatments

Three different heat treatments were carried out: conventional quenching, cryogenic treatment at -80 °C and cryogenic treatment at -196 °C. They are all presented in Table 2. The following tempering treatment was conducted at 250 °C for 1.5 hours.

Direct nebulization was applied for the cryogenic cooling. This technique consists of the nebulization of liquid nitrogen directly in a chamber using a fan. The latter allows a homogeneous temperature distribution to be obtained.

2.3. Characterization methods

The microstructure of the processed region was evaluated using optical microscopy (Olympus CX31). The flat surfaces of the samples were wet-sanded using silicon carbide papers

and polished to a 1 µm finish before being immersed in Marble etchant (10 g CuSO₄, 50 ml HCl and 50 ml H₂O) to reveal any martensite and carbides present within the DIN 1.4110 martensitic stainless steel microstructure.

Three micro-hardness maps of the martensitic stainless steel samples were measured using a Vickers microhardness tester (Tukon 2100 B) with a load of 1 kgf for 15 s.

Surface roughness measurements were performed with a stylus profilometer (MarSurf XCR20) as standard ISO 12085:1998 at a load of 0.02 N cut-off of 0.8 mm and stylus velocity of 0.5 mm.s⁻¹ (11218 point measurements). The roughness R_a (arithmetical average height (µm)), R_z (10-point height (µm)) and R_t (maximum height of the profile (µm)) values were measured²⁹.

2.4. Corrosion test

Polarization curves, obtained in AUTOLAB PGSTAT 302N Potentiostat/Galvanostat equipment, were used to characterize the corrosion resistance of DIN 1.4110 martensitic stainless steel in the as-received and heat-treated conditions (Table 2). Table 3 shows the parameters used to characterize the corrosion resistance.

2.5. Tribocorrosion test

Sliding ball-on-flat wear tests under dry conditions and in the presence of corrosive medium conditions (tribocorrosion) were carried out on the DIN 1.4110 martensitic stainless steel in the as-received condition and with heat treatments (Table 2). The tests were performed using a CETR Universal Material Tester (UMT) wear tester. The parameters used are shown in Table 4.

The conditions shown in Table 4 are necessary to evaluate the synergistic effect of corrosion and wear on the metal degradation^{6,15}. Despite the wear test parameters (viz. normal load, frequency and stroke length) being similar in order to compare the results, the studied parameters (Table 4) are different to those suggested by the standard ASTM G133-05: 2010¹⁶.

Mathew et al.¹⁵ performed their study with low normal load in the wear test to observe the synergistic effect of corrosion and wear. Other authors⁸ also proposed to study wear resistance with protective oxide films under low load values, because these films are brittle and thin; therefore, low

Table 2. Studied samples of DIN 1.4110 martensitic stainless steel.

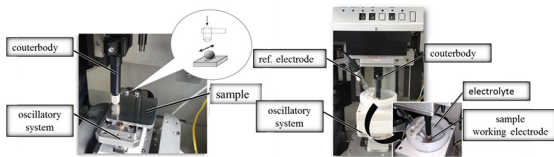
Sample	Heat Treatments
As Received	Process annealed (780 °C and cooled in air)
Conventional Quenching	1 hour at 1080 °C then air quenching. Following tempering treatment at 250 °C for 1.5 hours.
Cryogenic Treatment (-80 °C)	1 hour at 1080 °C then air quenching followed cryogenic treatment by direct nebulization in dry ice temperature (-80 °C) for 6 hours. Following tempering treatment at 250 °C for 1.5 hours.
Cryogenic Treatment (-196 °C)	1 hour at 1080 °C then air quenching followed cryogenic treatment by direct immersion into liquid nitrogen (-196 °C) for 6 hours. Following tempering treatment at 250 °C for 1.5 hours.

Table 3. Parameters used for potentiodynamic polarization tests.

Parameters	Details
Electrolyte	0.05 molL ⁻¹ NaCl
Open Circuit Potential (OCP) monitoring	30 min
Sweep range	-100 mV vs. OCP +600 mV vs. OCP
Scan Rate	1 mV.s ⁻¹
Reference electrode	Saturated calomel electrode (SCE)
Counter-electrode	Platinum

loads must be applied to study the synergistic wear-corrosion and repassivation of the passive film.

Figure 1 shows the ball-on-flat configuration for the dry test (a) and corrosive medium test (b). EG&G Princeton Applied Research (PAR) Potentiostat/Galvanostat equipment was used to monitor the open circuit potential (OCP) before, during, and after the wear tests (Figure 2). This methodology has been employed by other authors^{8,15}.

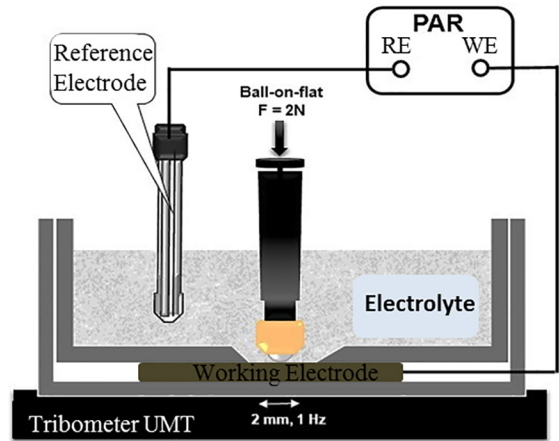
**Figure 1:** System ball-on-flat. a) dry Test and b) corrosive medium Test.

The worn volume was obtained according to the ASTM G133 - 05 (2010) standard¹⁶, section 9.3. Track profiles were acquired with a profilometer Bruker Contour GT-K. Then, the track area was measured using ImageJ software. Subsequently, the worn volume was calculated by multiplying this area by the stroke length.

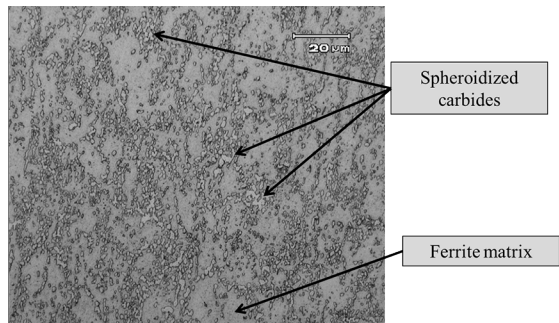
3. Results and discussion

3.1. Microstructure

After etching with Marble solution, the sample in the as-received condition shows a microstructure constituted

**Figure 2:** Schematic set-up for tribocorrosion tests.

by a ferrite matrix with spheroidized carbides (Figure 3), as expected⁹.

**Figure 3:** Microstructure of martensitic stainless steel DIN 1.4110 in the as received condition.

The sample quenched by the conventional heat treatment presents a microstructure composed of retained austenite and undissolved carbides distributed in a tempered martensitic matrix (Figure 4). This result has also been reported elsewhere^{2,9}.

Figures 5 and 6 show images of samples submitted to cryogenic quenching at -80 °C and -196 °C, respectively. The microstructures correspond to quenched and tempered martensite with the presence of dispersed carbides and a fraction of retained austenite, as reported by other authors¹⁷.

Table 4. Parameters used for wear tests.

Parameters	Dry Test	Corrosive Medium Test
Ball (4.76 mm diameter)	Alumina (Al ₂ O ₃)	Alumina (Al ₂ O ₃)
Normal Load	2 N	2 N
Frequency	1 Hz	1 Hz
Stroke Length	2 mm	2 mm
Room Temperature	20 - 23 °C	20 - 23 °C
Air Relative Humidity	50% - 60%	50% - 60%
Electrolyte	-	0.05 molL ⁻¹ NaCl
Reference Electrode	-	Saturated calomel electrode (SCE)

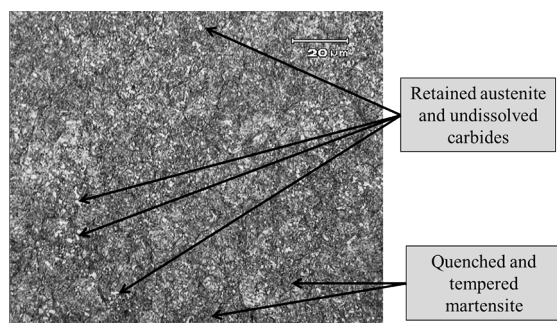


Figure 4: Microstructure of martensitic stainless steel DIN 1.4110 after quenching by conventional heat treatment and tempering at 250 °C for 1.5 h.

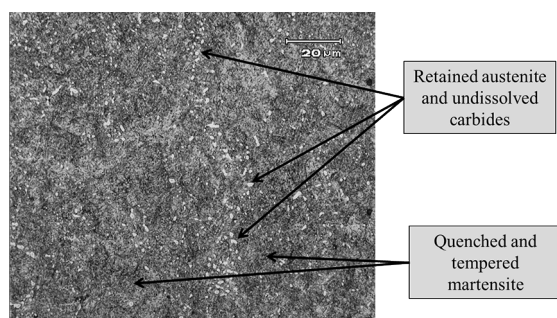


Figure 5: Microstructure of martensitic stainless steel DIN 1.4110 after cryogenic quenching at -80 °C and tempering at 250 °C for 1.5 h.

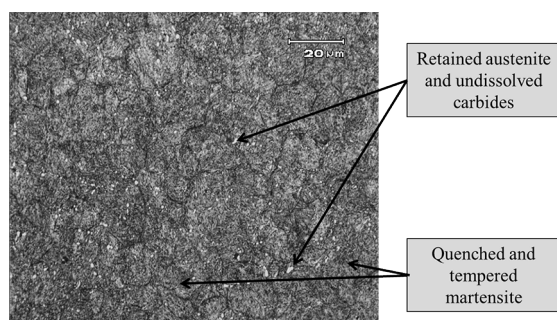


Figure 6: Microstructure of martensitic stainless steel DIN 1.4110 after cryogenic quenching at -196 °C and tempering at 250 °C for 1.5 h.

The retained austenite content was determined using image analysis software (ImageJ). The carbide amount was considered to be the same for the different heat treatments systems, and the reference sample corresponded to the as-received one. The sample quenched by the conventional heat treatment achieved 6.12% of retained austenite; the content of this phase for the cryogenic quenching down to -80 °C and -196 °C was 3.94% and 3.01%, respectively. This result points out that the cryogenic treatment promoted the formation of less retained austenite, crucial for good dimensional stability during service¹⁸.

Medium-chrome and medium/high-carbon steels present their martensite finish (M_f) line, independent of other factors, at roughly -120 °C¹⁹. Therefore, the sample submitted to

conventional heat treatment is far from the expected M_f temperature, which justifies the greater amount of retained austenite. The cryogenic heat treatment at -80 °C is closer to the expected M_f line; the treatment at -196 °C is probably under the M_f temperature. For the latter, the low air-cooling rate during the quenching process, and the interruption of the cooling to take the sample from air-cooling to cryogenic cooling, can promote the austenite stabilization²⁰. This explains the 3.01% of retained austenite in this sample, even when a temperature lower than M_f was achieved.

3.2. Hardness

The hardness values increase due to the structure modification promoted by the different heat treatments (Table 5). As mentioned before, the quenched and tempered samples have a tempered martensite structure and a percentage of retained austenite, whereas the as-received sample had a predominantly ferritic structure with spheroidized carbides.

Table 5. Vickers microhardness values for each kind of sample (1 kgf for 15 s).

Sample	Vickers microhardness
As received	201 ± 3.7
Conventional quenching	553 ± 11.2
Cryogenic quenching (-80 °C)	594 ± 6.3
Cryogenic quenching (-196 °C)	612 ± 8.5

According to Farina et al.²¹, carbides dissolve in the austenitization step, depending on the austenitizing temperature and time. Since these parameters were common for the different studied systems, the amount of dissolved carbides at high temperatures during austenitizing, it is reasonable to suppose that the final carbides content is similar among the three heat treatments employed. As a consequence, the hardness increase can be associated with the decrease in retained austenite, which agrees with the higher amount of martensite formed during the heat treatment.

3.3. Roughness

The samples' surface roughness values (Table 6), for all the samples after sanding with silicon carbide paper # 600, demonstrate the similar surface topography^{19,20}.

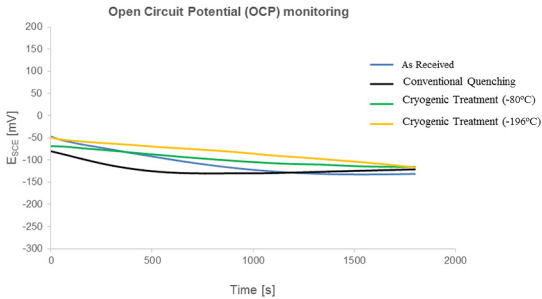
3.4. Electrochemical behavior

The open circuit potential was monitored for 30 minutes (Figure 7). All the samples developed very similar potential values.

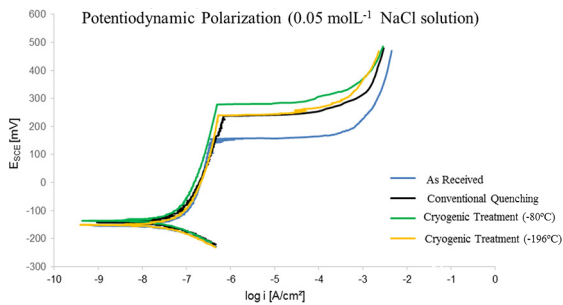
Figure 8 shows the potentiodynamic polarization curves obtained in 0.05 mol.L⁻¹ NaCl solution for all studied systems. Table 7 presents the results obtained from the potentiodynamic

Table 6. Surface roughness values.

Sample	Ra [μm]	Rz [μm]	Rt [μm]
As received	0.16 ± 0.04	1.19 ± 0.19	1.84 ± 0.38
Conventional quenching	0.14 ± 0.03	1.06 ± 0.19	1.73 ± 0.31
Cryogenic quenching (-80 °C)	0.15 ± 0.03	1.13 ± 0.20	1.61 ± 0.31
Cryogenic quenching (-196 °C)	0.13 ± 0.01	0.97 ± 0.08	1.64 ± 0.06

**Figure 7:** OCP monitoring in a 0.05 molL^{-1} NaCl solution.

polarization curves, including the corrosion potential (E_{corr}) and corrosion current (i_{corr}) obtained by Tafel extrapolation using Nova® software, pitting potential (E_{pit}), as well as the passivation potential range (ΔE_{pass}). The latter can be read directly on the polarization curve, or calculated from the subtraction of E_{corr} from E_{pit} .

**Figure 8:** Potentiodynamic polarization curves in a 0.05 M NaCl solution; -100 mV vs. OCP to +600 mV vs. OCP; 1 mV.s-1.

All polarization curves develop the same profile (Figure 8), which reveals the same corrosion behavior. The Tafel extrapolation values (Table 7) demonstrate the decrease of i_{corr} for the heat-treated samples. However, deep heat treatment is not steadily gaining acceptance as a process for

Table 7. Tafel extrapolation results, pitting and passive region.

Sample	E_{corr} [mV]	i_{corr} [$\text{A}\cdot\text{cm}^{-2}$]	E_{pit} [mV]	ΔE_{pass} [mV]
As received	-152	1.9×10^{-07}	142	294
Conventional quenching	-142	4.3×10^{-08}	236	378
Cryogenic quenching (-80°C)	-136	4.8×10^{-08}	273	409
Cryogenic quenching (-196°C)	-152	6.6×10^{-08}	240	392

improving the corrosion resistance, as reported by Uygur et al.²¹. There is an improvement in the corrosion resistance, considering both the general and pitting corrosion, the latter being the kind of corrosion that too often attacks this class of steel²². Steels submitted to the quenching and tempering processes have a higher pitting potential than the as-received one. The increase in the pitting potential involved a more important passivation potential range. This behavior may be related to the decrease of spheroidized carbides amount compared to the as-received steel (Figure 3). Carbides may work as preferential sites for pitting corrosion initiation¹⁴.

The amount of retained austenite in the studied martensitic stainless steel DIN 1.4110 does not influence the corrosion potential, nor the pitting potential, as can be seen in Figure 8, and reported by Kimura et al.²³. This is the reason why no significant alteration of these values was observed among the different heat treatments applied and, as a consequence, among the different amounts of retained austenite in each microstructure (Figures 4-6).

3.5. Tribocorrosion behavior

Friction coefficient (COF) values were monitored for all the samples under dry conditions and in a corrosive medium (Table 8).

In the dry conditions, the COF values were similar for all the samples. The same behaviors were obtained in corrosive conditions. This means that the different heat treatments do not have a significant effect on this response (COF) for this type of martensitic stainless steel.

Tests conducted in the corrosive medium yielded COF values lower than those obtained for the dry conditions, since the sodium chloride solution works simultaneously with the electrolyte and as a surface lubricant. However, the reduction of COF does not necessarily involve a wear resistance increase; the presence of the electrolyte enhances the material loss probably by the corrosion process, indicating the synergistic wear-corrosion effect⁸. From Figures 9-13,

Table 8. COF values for all the samples for dry and corrosive conditions.

Sample	COF	
	Dry	Corrosive medium
As received	0.80 ± 0.3	0.39 ± 0.2
Conventional quenching	0.72 ± 0.1	0.40 ± 0.2
Cryogenic quenching (-80°C)	0.73 ± 0.1	0.37 ± 0.3
Cryogenic quenching (-196°C)	0.72 ± 0.2	0.40 ± 0.1

it is possible to observe that the worn volume was higher than in the dry conditions, independent of the system. These results show that wear in the presence of a corrosive medium for martensitic stainless steel DIN 1.4110 is an aggressive condition for the material's integrity. Since chloride-containing media are very common in cutlery and the food industry²⁴, wear can strongly compromise the components' integrity.

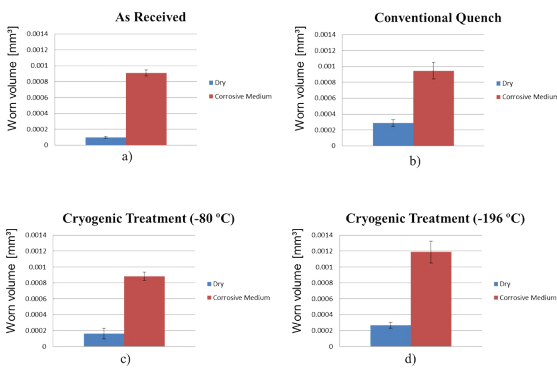


Figure 9: Worn volume loss for tests in dry condition and in presence of corrosive medium for all the conditions: a) As received, b) conventional quenching, c) cryogenic quenching (-80 °C), d) cryogenic quenching (-196 °C).

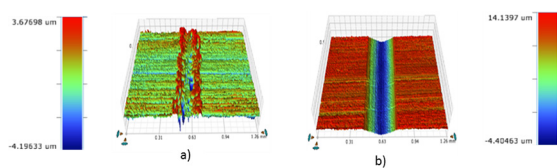


Figure 10: Profilometry results for the as-received sample in a) dry condition and b) corrosive medium.

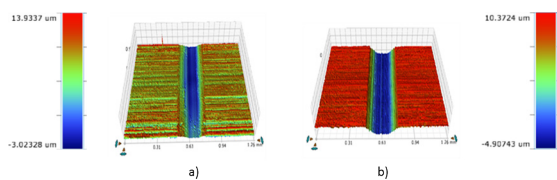


Figure 11: Profilometry results for the conventional quenching sample in a) dry condition and b) corrosive medium.

Dodds et al.⁹ studied wear on a friction stir welding process applied on martensitic AISI 420 stainless steel. They compared three different layers from the surface towards the

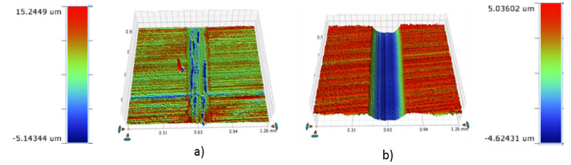


Figure 12: Profilometry results for the cryogenic quenching (-80 °C) sample in a) dry condition and b) corrosive medium.

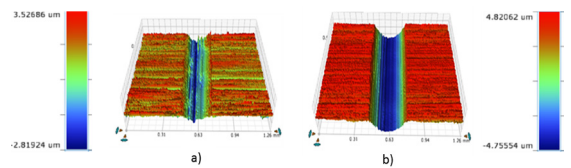


Figure 13: Profilometry results for the cryogenic quenching (-196 °C) sample in a) dry condition and b) corrosive medium.

material bulk in the as-received condition; then, they submitted the steel to the conventional quenching and tempering heat treatments, and verified the influence of the heat input. This is why they used a ball-on-flat system (the configuration also used here), as a wear test; based on the track dimensions, they obtained the worn volume reduction and compared the heat-treated steel to the spheroidized steel. They achieved a reduction in the track width of 40 % for the heat-treated steel. Here, however, a similar approach was followed, yet the result was not similar. The difference between the results can be explained by the load employed in each test: since the aim of this study was to evaluate the tribocorrosion performance of the samples with their respective heat treatments, the applied load was not as high as that proposed by Dodds et al.⁹; other studies¹⁵ suggest the application of low normal forces when in a corrosive solution. The role of the load in tribocorrosion test is associated with the removal of the passive film and its following repassivation. Low loads allow the role of the corrosive medium in the degradation process to be evaluated in the form of corrosion-wear synergistic. Meanwhile, the wear test under dry conditions shows purely mechanical wear.

Although the heat treatments improve the corrosion resistance of the studied material (Figure 8), they do not modify the steel's behavior under tribocorrosion conditions where the synergistic effects of corrosion and wear are present (Figure 9). A very similar volume loss for all the samples was observed in the corrosive medium. It should be noted

that, in this kind of steel, the heat treatment has as its main function an increase in the hardness and wear resistance to enhance the tribocorrosion resistance.

Figure 14 presents optical micrographs of the wear tracks of the samples in dry and medium conditions. Figure 14a shows plastic deformation and debris bed on the track for the as-received sample. This suggests the predominant mechanism of plowing²⁸ for this sample; meanwhile, for the heat-treated steels, the wear mechanism corresponded to cutting. For this reason, the worn volume for the as-received sample is difficult to determine (Figure 9a), and was less than expected.

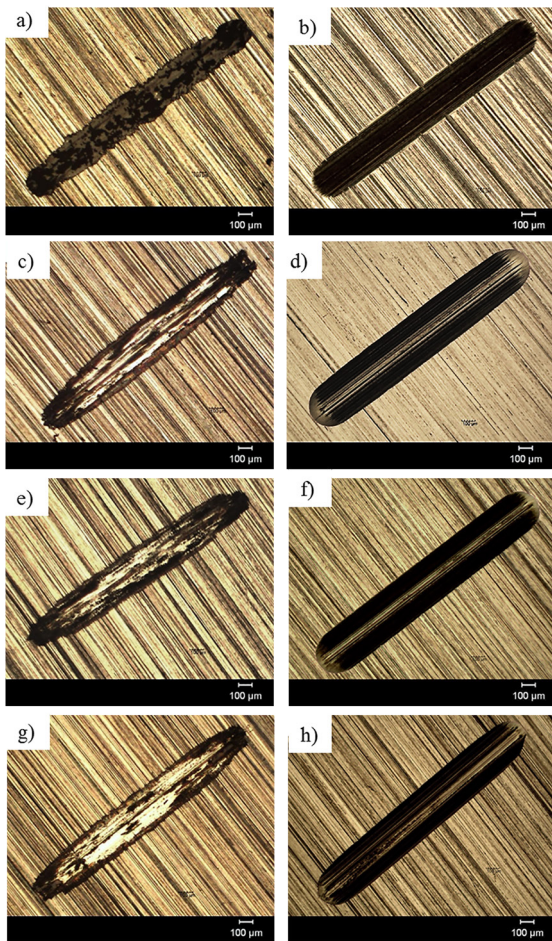


Figure 14: Optical microscopy of the worn tracks. a) As Received in dry condition; b) As Received in corrosive medium; c) Conventional Quenching in dry condition; d) Conventional Quenching in corrosive medium; e) Cryogenic Treatment (-80 °C) in dry condition; f) Cryogenic Treatment (-80 °C) in corrosive medium; g) Cryogenic Treatment (-196 °C) in dry condition; e h) Cryogenic Treatment (-196 °C) in corrosive medium.

The presence of a debris bed on the as-received steel after the wear test (Figure 14a) could be caused by the oxide formation (darkest track on Figure 14a). This sample contains the highest carbide percentage, including chromium carbides. This reduces the amount of chromium available to

form a passive layer. On the other hand, for the same steel condition after the tribocorrosion test, the sodium chloride medium influenced the wear mechanism, changing from plowing to cutting.

The corrosion protection mechanism of stainless steels is based on surface passivation (Figure 8). This is the formation of a thin, adherent and dense chromium oxide layer on the steel surface³ in air atmosphere. During the wear test, the ball in relative movement removes the chromium oxide layer and exposes the steel to the aggressive environment, which is confirmed by the decrease of the free potential values in Figure 15.

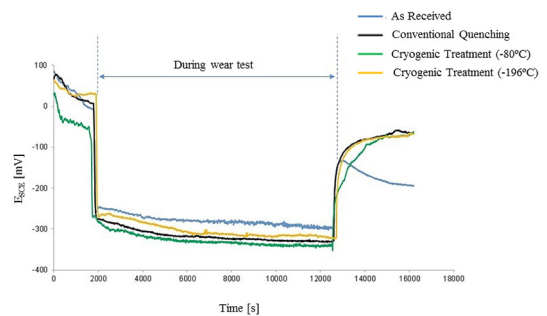


Figure 15: Open circuit potential monitoring results before, during and after wear test.

In the tribocorrosion tests, the sliding velocity is important because it may influence the repassivation process. When the ball slides on the surface, more active material is exposed to the electrolyte; but while the ball removes the passive film, the chromium oxide layer forms again (repassivation) on the opposite side of the track. This cycle of rupture, corrosion and regeneration of the passive film brought about the increase in the worn volume (Figure 9). Moreover, wear is more aggressive in a corrosive medium, although the latter can also work as a lubricant fluid (Table 8)⁸. The as-received steel, which has the lowest hardness, and the sample after -196 °C cryogenic quenching (the hardest sample), both show close worn volume values. In order to explain these results, further studies are necessary, because the results obtained here did not allow us to determine the causes of these different and unexpected behaviors.

Samples of spheroidized steel developed an important potential decrease after the tribocorrosion test (Figure 15). This behavior could be associated with the presence of spheroidized carbides (Figure 3). The carbides are preferential sites for the corrosion process and hamper passivation, as already mentioned.

4. Conclusions

Our results can be summarized as follows:

- The microstructure is dependent on the heat treatment parameters employed. A decrease in the content of

retained austenite was observed, as a function of the final quenching cooling temperature: 6.12% for conventional quenching, 3.94% for -80 °C quenching and 3.01% for -196 °C quenching. These results are coherent with the Vickers microhardness results.

- All the heat-treated samples showed a decrease of i_{corr} and an increase of pitting potential, compared to the as-received samples. Consequently, the heat treatments extended the passive region (ΔE_{pass}). The martensite-rich samples therefore have a better corrosion resistance than the spheroidized ones. Worn volume is higher for the tribocorrosion tests than for the wear test under dry conditions.
- The sample obtained by cryogenic heat treatment at -196 °C promoted the highest amount of worn volume under tribocorrosion conditions. The sample that went through cryogenic heat treatment at -80 °C yielded almost the same worn volume as the conventional heat-treated sample.

5. Acknowledgments

Authors gratefully thank the financial support of the Brazilian Government Agencies CAPES (Agency for Support and Evaluation of Graduate Education) and CNPq (National Counsel of Technological and Scientific Development).

6. References

- Verhoeven JD, Pendray AH, Clark HF. Wear tests of steel knife blades. *Wear*. 2008;265(7-8):1093-1099.
- ASM International. *ASM Handbook Volume 3: Alloy Phase Diagrams*. Materials Park: ASM International; 1992.
- Sedriks AJ. *Corrosion of stainless steels*. 2nd ed. New York: John Wiley and Sons; 1996.
- Khajavi MR, Shariat MH. Failure of first stage gas turbine blades. *Engineering Failure Analysis*. 2004;11(4):589-597.
- Xi YT, Liu DX, Han D. Improvement of corrosion and wear resistances of AISI 420 martensitic stainless steel using plasma nitriding at low temperature. *Surface and Coatings Technology*. 2008;202(12):2577-2583.
- Li CX, Bell T. Corrosion properties of plasma nitrided AISI 410 martensitic stainless steel in 3.5% NaCl and 1% HCl aqueous solutions. *Corrosion Science*. 2006;48(8):2036-2049.
- Lo KH, Shek CH, Lai JKL. Recent developments in stainless steels. *Materials Science and Engineering: R: Reports*. 2009;65(4-6):39-104.
- Berradja A, Bratu F, Benea L, Willems G, Celis JP. Effect of sliding wear on tribocorrosion behaviour of stainless steels in a Ringer's solution. *Wear*. 2006;261(9):987-993.
- Dodds S, Jones AH, Cater S. Tribological enhancement of AISI 420 martensitic stainless steel through friction-stir processing. *Wear*. 2013;302(1-2):863-877.
- Barron RF. Cryogenic treatment of tool steels. *Manufacturing Strategies*. 1996;6:535-548.
- Molinari A, Pellizzari M, Gialanella S, Straffelini G, Stiasny KH. Effect of deep cryogenic treatment on the mechanical properties of tool steels. *Journal of Materials Processing Technology*. 2001;118(1-3):350-355.
- Barron RF. Cryogenic treatment of metals to improve wear resistance. *Cryogenics*. 1982;22(8):409-413.
- Podgornik B, Majdic F, Leskovsek V, Vizintin J. Improving tribological properties of tool steels through combination of deep-cryogenic treatment and plasma nitriding. *Wear*. 2012;288:88-93.
- Isfahany AN, Saghafian H, Borhani G. The effect of heat treatment on mechanical properties and corrosion behavior of AISI420 martensitic stainless steel. *Journal of Alloys and Compounds*. 2011;509(9):3931-3936.
- Mathew MT, Runa MJ, Laurent M, Jacobs JJ, Rocha LA Wimmer MA. Tribocorrosion behavior of CoCrMo alloy for hip prosthesis as a function of loads: A comparison between two testing systems. *Wear*. 2011;271(9-10):1210-1219.
- ASTM International. *ASTM G133-05. Standard Test Method for Linearly Reciprocating Ball-on-Flat Sliding Wear*. West Conshohocken: ASTM International; 2010.
- Rhyim YM, Han SH, Na YS, Lee JH. Effect of Deep Cryogenic Treatment on Carbide Precipitation and Mechanical Properties of Tool Steel. *Solid State Phenomena*. 2006;118:9-14.
- Sidoroff C, Perez M, Dierickx P, Girodin D. Advantages and Shortcomings of Retained Austenite in Bearing Steels: a Review. In: Beswick J. *Bearing Steel Technologies: 10th Volume, Advances in Steel Technologies for Rolling Bearings*. West Conshohocken: ASTM International; 2014. p. 1-37.
- Barlow LD, Du Toit M. Effect of Austenitizing Heat Treatment on the Microstructure and Hardness of Martensitic Stainless Steel AISI 420. *Journal of Materials Engineering and Performance*. 2012;21(7):1327-1336.
- Roberts G, Kennedy R, Krauss G. *Tool Steels*. 5th ed. West Conshohocken: ASM International; 1998.
- Farina PFS, Farina AB, Barbosa CA, Goldenstein H. Tratamento criogênico e de alívio de tensões em um aço AISI D2. *Tecnologia em Metalurgia, Materiais e Mineração*. 2012;9(2):140-147.
- Hilbert LR, Bagge-Ravn D, Kold J, Gram L. Influence of surface roughness of stainless steel on microbial adhesion and corrosion resistance. *International Biodeterioration & Biodegradation*. 2003;52(3):175-185.
- Sedlaček M, Podgornik B, Vizintin J. Influence of surface preparation on roughness parameters, friction and wear. *Wear*. 2009;266(3-4):482-487.
- Uygun I, Gerengi H, Arslan Y, Kurtay M. The Effects of Cryogenic Treatment on the Corrosion of AISI D3 Steel. *Materials Research*. 2015;18(3):569-574.
- Frankel GS. Pitting Corrosion of Metals. A Review of the Critical Factors. *Journal of The Electrochemical Society*. 1998;145(6):2186-2198.

26. Kimura M, Miyata Y, Toyooka T, Kitahaba Y. Effect of Retained Austenite on Corrosion Performance for Modified 13%Cr Steel Pipe. *Corrosion*. 2001;57(3):433-439.
27. Hidalgo PJ. Pitting corrosion of martensitic cutlery steels. *Surface Technology*. 1980;10(3):193-208.
28. Ravi N, Markandeya R, Joshi SV. Effect of substrate roughness on adhesion and tribological properties of nc-TiAlN/a-Si₃N₄ nanocomposite coatings deposited by cathodic arc PVD process. *Surface Engineering*. 2015;33(1):7-19.
29. Gadelmawla ES, Koura MM, Maksoud TMA, Elewa IM, Soliman HH. Roughness parameters. *Journal of Materials Processing Technology*. 2002;123(1):133-145.